Chlorophyll-*a* variability off Patagonia based on SeaWiFS data

Silvia I. Romero,[1,2] Alberto R. Piola,[1,2,3] Marcela Charo,[1] and Carlos A. Eiras Garcia[4]

Received 23 August 2005; revised 7 December 2005; accepted 27 February 2006; published 27 May 2006.

[1] Seasonal to interannual variability of satellite derived chlorophyll-*a* over the Patagonia shelf and shelf break in the western South Atlantic are studied based on 7 years of ocean-color data (1998–2004) from the Sea-Viewing Wide Field-of-View Sensor (SeaWiFS). Strong chlorophyll-*a* seasonal variability (>4 mg m^{-3}) is observed compared to the open ocean (<1.5 mg m^{-3}). North of 45°S, chlorophyll-*a* blooms initiate in early austral spring (September and October), while south of 45°S blooms begin in late spring to early summer (November through January). The spring maximum (>3.5 mg m^{-3}) extends from the midshelf to the shelf break between 37°S and 44°S and southward to 51°S along a narrow shelf break band. In summer the shelf break maximum persists from 37°S to 51°S, and two inner-shelf blooms develop off Valdés Peninsula and along a near-coastal band between 46°S and 52°S (>3 mg m^{-3}). Chlorophyll-*a* concentrations in the northern midshelf sharply decay in late spring, reaching lowest concentrations in summer (February and March) and a secondary maximum in early winter (June). Though all regions present substantial interannual variations, the bloom locations are stable. The shelf break maximum is located inshore of the front between the low salinity shelf waters and the cold, salty, and nutrient-rich Malvinas Current waters. The inner shelf maxima are offshore of fronts separating well-mixed coastal waters from the stratified midshelf. North of 41°S the midshelf bloom is also associated to a bottom trapped thermal front. Thus, all the high chlorophyll-*a* regions are associated to well-defined fronts.

Citation: Romero, S. I., A. R. Piola, M. Charo, and C. A. E. Garcia (2006), Chlorophyll-*a* variability off Patagonia based on SeaWiFS data, *J. Geophys. Res.*, *111*, C05021, doi:10.1029/2005JC003244.

1. Introduction

[2] South of about 40°S the western South Atlantic presents a wide continental shelf referred to as the Patagonia shelf. The region is part of a large marine ecosystem supporting an extraordinary rich and diverse community of species attracted by high concentrations of plankton. Some of the fish and squid species are of major regional or global commercial importance [*Food and Agricultural Organization (FAO)*, 1994]. The relatively flat Patagonia shelf (slope ~1:1000) widens southward from about 170 km at 39°S to 850 km at 50°S (Figure 1). The most distinguishable morphological features are four terraces of variable width, with shelves at 25–30 m, 85–100 m, 110–120 m (between 43°S and 50°S) and 130–150 m [*Parker et al.*, 1997]. To the east the shelf terminates in a sharp break with a mean slope of 1:50, its width varying between 50 and 300 km and intersected by approximately 50 canyons of variable width and depth [*Mouzo*, 1982]. The shelf break is located between 110 and 165 m depth [*Parker et al.*, 1997].

[3] The shelf is occupied by diluted subantarctic waters derived from the southeast Pacific, a region subject to substantial continental runoff and excess precipitation over evaporation. The lowest salinities (~32) on the Patagonia shelf are observed around the eastern mouth of the Strait of Magellan [*Brandhorst and Castello*, 1971; *Guerrero and Piola*, 1997]. Salinity progressively increases northeastward and offshore, reaching about 33.8 at the shelf break, suggesting a northeastward mean flow over the inner and midshelf regions, referred to as the Patagonian Current [*Brandhorst and Castello*, 1971]. Salinity presents relatively small seasonal and vertical variations, however, warming in the late spring and early summer induce strong vertical stratification over the mid and outer shelf. In response to heat lost to the atmosphere and wind mixing, the continental shelf stratification begins weakening in early March and by late June the seasonal thermocline and pycnocline are eroded [*Rivas and Piola*, 2002]. Enhanced vertical mixing due to the interaction of strong tidal currents with the ocean bottom lead to much weaker stratification in the inner shelf [*Glorioso*, 1987; *Bianchi et al.*, 2005]. The vorticity balance from high resolution numerical simulations reveals that tidal current induced mixing is also important in arresting cross-isobath flows, which may lead to the development of upwelling and downwelling regions [*Palma et al.*, 2004]. The only available direct long-term current observations

[1]Departamento Oceanografía, Servicio de Hidrografía Naval, Buenos Aires, Argentina.
[2]Also at Departamento Ciencias de la Atmósfera y los Océanos, Facultad de Ciencias Exactas y Naturales, Universidad de Buenos Aires, Buenos Aires, Argentina.
[3]Also at Consejo Nacional de Investigaciones Científicas y Técnicas, Argentina.
[4]Departamento de Física, Fundação Universidade Federal do Rio Grande, Rio Grande, Brazil.

0148-0227/06/2005JC003244

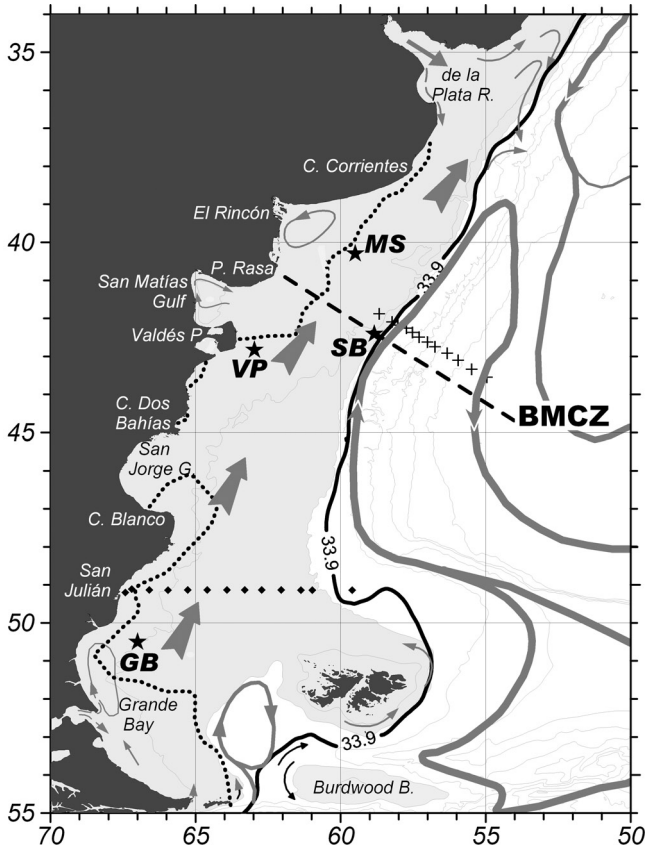

Figure 1. Schematic surface circulation in the western South Atlantic shelf (adapted from *Piola and Rivas* [1997] and *Sabatini et al.* [2004]). The stars indicate the four locations selected to depict the time series of Figure 3 at the midshelf (MS), shelf break (SB), Valdés Peninsula (VP), and Grande Bay (GB). The Brazil/Malvinas Confluence Zone (BMCZ) is indicated. Also shown are the locations of hydrographic sections presented in Figures 8 (diamond) and 9 (cross). The heavy line is the surface outcrop of the 33.9 isohaline and the heavy dashed line indicates the section used to prepare the space-time plot of Figure 4. The dotted line is the summer location of the Simpson stability parameter 50 J m^{-3}, adapted from *Lucas et al.* [2005] and *Bianchi et al.* [2005]. Thin contours correspond to the 100, 200 (shaded), 1000, 2000, 3000, 4000, and 5000 m isobaths.

suggest that the flow over the shelf is dominated by tidal and inertial oscillations and a relatively weak mean current toward the north northeast [*Piola and Rivas*, 1997; *Rivas*, 1997]. A northeastward mean flow over the shelf is also derived from models of varying complexity [e.g., *Forbes and Garraffo*, 1988; *Glorioso and Flather*, 1995; *Palma et al.*, 2004].

[4] The intense Malvinas Current flows northward along the eastern margin of the continental shelf, advecting nutrient rich subantarctic waters from the northern Drake Passage into the western Argentine Basin up to 38°S. The Malvinas Current forms a cyclonic wedge (Figure 1) frequently trapping cold-fresh and nutrient rich Polar Front waters east of the northward flowing branch [*Piola and Gordon*, 1989]. The transition between shelf and Malvinas Current waters, characterized by moderate cross-front temperature and salinity gradients, is here referred to as the shelf break front.

[5] Analysis of summer in situ data first suggested the existence of patches of high chlorophyll-*a* (chl-*a* > 3–5 mg m^{-3}) west of the core of the Malvinas Current, and much lower values in winter [*Brandhorst and Castello*, 1971]. We refer to this band as the Patagonia High Chlorophyll Band (PHCB). Coastal Zone Color Scanner (CZCS) data later revealed that the region of high chlorophyll forms a quasi-continuous band located close to the shelf break during the austral spring and summer [*Podestá*, 1988, 1997; *Longhurst*, 1998]. High chl-*a* concentrations (16 mg m^{-3}) observed in the outer continental shelf have been related to unusual dinoflagellate blooms [*Negri et al.*, 1992]. *Brown and Podestá* [1997] proposed that the high-reflectance patches observed in surface waters of the shelf and beyond were blooms of the coccolithophore *Emiliania huxleyi*. The analysis of 5 years of weekly SeaWiFS images has revealed that the shelf break zone is characterized by a strong annual cycle in satellite derived surface chlorophyll-a [*Garcia et al.*, 2004]. The shelf break region is important for the life cycle of several economically important species [*Podestá*, 1988; *Bertolotti et al.*, 1996; *Sánchez and Ciechomski*, 1995; *Rodhouse et al.*, 2001; *Acha et al.*, 2004; *Bogazzi et al.*, 2005]. There are also reports of high chlorophyll concentrations in the inner shelf off Valdés Peninsula in spring [*Carreto et al.*, 1986]. In addition, in situ data collected in summer and fall 2000–2004 present a wide midshelf region of high chl-*a* extending from 45°S to the southern tip of South America [*Bianchi et al.*, 2005]. The summer-fall blooms of southern Patagonia occur offshore of a series of near-coastal fronts which also bound regions of high CO_2 uptake from the atmosphere [*Bianchi et al.*, 2005]. These results suggest that vertical stratification plays a key role in determining the CO_2 fluxes. Several studies suggest that the Patagonian shelf presents large satellite derived chl-*a* variability compared to other ocean regions [e.g., *Gregg and Conkright*, 2002; *Dandonneau et al.*, 2004; *Gregg et al.*, 2005]. Yet, the structure of the chl-*a* distribution, its seasonal and longer timescale variations and the nutrient enrichment mechanisms that maintain these ecosystems are poorly understood. The purpose of this article is to describe the seasonal and interannual variability of the high chl-*a* regions of the southwestern South Atlantic continental shelf and their relations to the thermohaline structures over the seven year period. The analysis is based on satellite derived ocean color and historical hydrographic data, both described in section 2. The seasonal and interannual variability are presented in section 3 and the discussion and conclusions in sections 4 and 5, respectively.

2. Data and Methods

2.1. Satellite Data

[6] We used Standard Mapped Images (SMI) of monthly satellite derived chl-*a* concentrations, from the Sea-viewing Wide Field-of-view Sensor (SeaWiFS) for the period 1998–2004. Following *Yoder* [2000], the satellite-derived sea surface chl-*a* concentration is hereafter referred to as CSAT. CSAT data were estimated after NASA's reprocessing 4

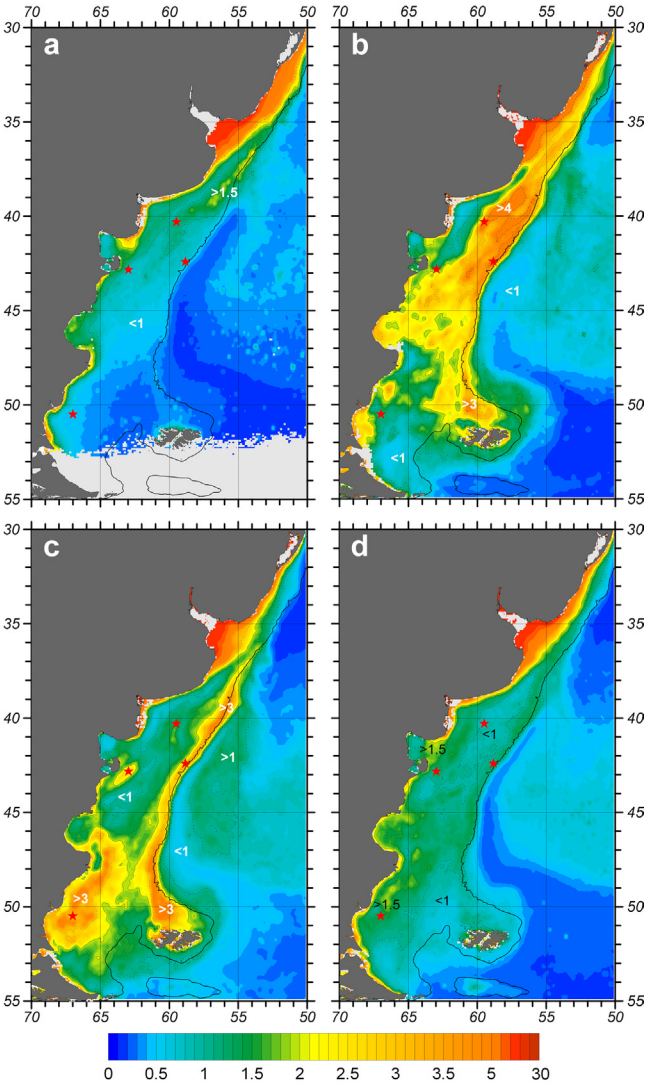

Figure 2. SeaWiFS derived surface chl-*a* (mg m^{-3}) in (a) austral winter (JJA), (b) spring (SON), (c) summer (DJF), and (d) fall (MAM) in the western South Atlantic. The red stars indicate the locations selected to analyze the time variability. The solid black line is the 200 m isobath. The light gray shading shows areas where cloud cover exceeds 30% of the total number of months and areas where CSAT values exceed 64 mg m^{-3}.

[*Patt et al.*, 2003] and 4.1 for the periods 1998–2002 and 2003–2004, respectively. CSAT estimates after reprocessing 4 and 4.1 are not significantly different [*Feldman and McClain*, 2005]. The SMIs are derived from Level-3 monthly binned data and mapped over a global two-dimensional array of Equidistant Cylindrical projection of 0.09° × 0.09° resolution. In the present analysis the global SMI data were subsampled to the region bounded by 22–62°S and 33–77°W (463 by 507 pixels). CSAT concentrations are in mg m^{-3}.

[7] In addition, for the year 2001 and for 25 September 1997, we used 1.1 km × 1.1 km resolution SeaWiFS Local Area Coverage (LAC) data obtained at High Resolution Picture Transmission (HRPT) Ground Stations located in Argentina and Brazil. The LAC data from 25 September 1997 were analyzed in conjunction with hydrographic data while the 2001 data were used to evaluate the merit of the SMI product to capture the CSAT regional patterns from monthly to interannual timescales. These LAC data were processed based on the OC4v4 bio-optical algorithm [*O'Reilly et al.*, 1998] using the SeaWiFS Data Analysis System software (SeaDAS v.4.1 and v.4.6). OC4v4 estimates CSAT with a high level of accuracy over the wide range that exists in the global ocean [*O'Reilly et al.*, 1998]. Recent studies carried out in the western South Atlantic have shown that OC4v4 based CSAT estimates are generally in good agreement with in situ bio-optical observations in the open ocean [*Garcia et al.*, 2005] and also at a near-coastal location [*Lutz et al.*, 2006]. The lack of sufficient spatial and temporal satellite data coincidental with in situ observations was compensated by comparing the derived patterns with historical in situ chl-*a* data (primarily from *Brandhorst and Castello* [1971], *Carreto et al.* [1995], and *Brandini et al.* [2000]).

[8] Using a centered difference scheme we also computed sea surface temperature (SST) gradients based on 13 years (1985–1997) of satellite data of the Pathfinder+Erosion monthly climatology of 9.28 km × 9.28 km resolution [*Casey and Cornillon*, 1999, 2001].

2.2. Hydrographic Data

[9] We analyzed hydrographic data collected in February 1967, March 1994, March 1996, and September 1997 across the Patagonia shelf break. In February 1967 the nominal station separation was 40 km and the data were collected at discrete levels. The latter cruises were designed to explore the cross-front density structure with closely spaced stations (~20 km) using quasi-continuous conductivity-temperature-depth (CTD) profilers. Detailed descriptions of the hydrographic conditions over the shelf are available elsewhere [see *Carreto et al.*, 1986; *Carreto et al.*, 1995; *Guerrero and Piola*, 1997; *Sabatini and Martos*, 2002; *Bogazzi et al.*, 2005, and references therein].

3. Analysis

3.1. Seasonal Variability

[10] The 1998–2004 mean seasonal CSAT distributions are presented in Figure 2. Throughout the year CSAT is higher over the mid and outer shelf than in the open ocean. Most of the middle and outer shelf areas undergo a seasonal CSAT cycle of large amplitude, with lowest concentrations in winter (JJA, <1 mg m^{-3}) and highest concentrations (>3 mg m^{-3}) in spring (SON) or summer (DJF). Figure 2 reveals that the seasonal changes in chl-*a* described from in situ observations at the shelf break [*Brandhorst and Castello*, 1971], off Cape Corrientes [*Carreto et al.*, 1995], and northern Patagonia [*Carreto et al.*, 1986] are local manifestations of wider-scale regional patterns of chl-*a* distribution. A large midshelf region located between 37 and 44°S presents relatively high CSAT (~1.5 mg m^{-3}) in winter compared to neighboring regions and elsewhere away from near-coastal locations (Figure 2a). West of this local maximum, off El Rincón, CSAT is low throughout the year (Figure 2). The highest monthly mean CSAT values in this region (~1.2 mg m^{-3}) are observed in May and the lowest (0.5 mg m^{-3}) in November (not shown). In some

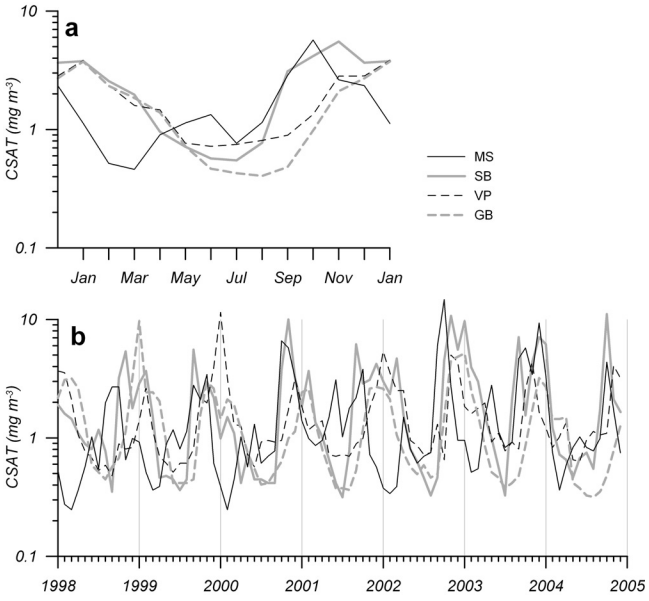

Figure 3. The 1998–2004 SeaWiFS derived surface chl-*a* (mg m^{-3}) (a) monthly mean climatology and (b) time series at the midshelf (MS, thin solid line), shelf break (SB, heavy solid line), off Valdés Peninsula (VP, thin dashed line), and Grande Bay (GB, heavy dashed line). Each January is indicated by a vertical line in Figure 3b.

near-coastal locations, which are more clearly distinguished in winter, the CSAT signal is contaminated by dissolved and suspended organic and inorganic matter derived from river discharges. The continental discharge effect is extensive near the Río de la Plata (Figure 2a) [see *Framiñan and Brown*, 1996; *Piola and Romero*, 2004; *Huret et al.*, 2005] but also occurs in a smaller scale in Patagonian rivers of reduced outflow. In addition, high CSAT concentrations (>2 mg m^{-3}) in winter are apparent east of San Matías Gulf. Over most of the middle and outer shelf the major bloom occurs in spring (Figure 2b). In November, the most productive month over the shelf break, the bloom forms a narrow band (25–40 km) extending 1500 km from ~38° to 51°S, closely following the 150–200 m isobaths. Mean CSAT concentrations off Grande Bay are higher in summer than in spring. The delayed bloom in the inner shelf of southern Patagonia is also apparent in seasonal chlorophyll distributions derived from CZCS [*Longhurst*, 1998] and in coarse resolution global analyses for 1998–2001 [*Dandonneau et al.*, 2004, Figure 4]. In this region, north of 52°S and extending to about 46°S, a high CSAT band (>3 mg m^{-3}) located ~50 km from the coast is observed in summer. In summer, north of 47°S CSAT decays to values lower than 1 mg m^{-3} in the midshelf but remains high (>3 mg m^{-3}) throughout the shelf break and east of Valdés Peninsula (Figure 2c). Analysis of monthly mean distributions (not shown) reveals that the spring bloom begins in September at the shelf break north of 45°S, while off Grande Bay the bloom begins in November. In the fall (MAM) CSAT decays sharply in the midshelf while localized relative maxima (1–1.5 mg m^{-3}) are still observed at the shelf break, off San Matías Gulf, Cape Blanco, and San Julián (Figure 2d).

[11] The seasonal CSAT distributions (Figure 2) reveal several localized maxima. Within these regions, four locations are selected to further investigate the monthly CSAT variability (Figure 3). Three of these locations are from northern Patagonia: off Valdés Peninsula (VP), at the midshelf (MS), and at the shelf break (SB), within the core of the PHCB. The fourth location is off Grande Bay (GB) in southern Patagonia. At SB, MS, and GB, and over most of the shelf, the highest CSAT concentrations are observed in late spring (October and November), though the spring bloom at MS occurs on average 1 month earlier than at SB. At VP and off Cabo Blanco (not shown) the bloom is observed in summer (December–January). The CSAT seasonal variations at MS are distinct from all other regions. After the spring bloom CSAT at MS and throughout the mid-shelf region rapidly decays to ~0.5 mg m^{-3} (Table 1, Figure 2c). In fact, on average, the lowest concentrations at MS occur in February through March, when the SB still presents substantial CSAT concentrations (>2 mg m^{-3}). Also in contrast with all other regions MS presents increased CSAT concentrations in June (Figure 3a). Finally, it is noted that the rapid spring CSAT increase at GB, SB, and MS (~3 mg m^{-3} per month) is in contrast with the slow decay at GB, SB, and VP (Figure 3a). On the basis of the CSAT monthly mean climatology, Table 1 summarizes the amplitude (CSAT max − CSAT min) and month of highest and lowest CSAT concentration at the selected sites and, for comparison, three additional locations: in the southern part of the PHCB, off San Julián and a midshelf site, referred to as "open shelf," located at 45°S away from high CSAT regions.

3.2. Interannual Variability

[12] The 1998–2004 CSAT monthly time series reveal significant and complex year to year variability (Figure 3b). At all selected locations the low CSAT values are relatively uniform, within 0.3 to 0.8 mg m^{-3}, but the amplitude and timing of the blooms are highly variable. For instance, at SB CSAT reached 5.4 mg m^{-3} in November 1998 and 11.1 mg m^{-3} in October 2004. In contrast, at GB the highest CSAT concentration was almost 10 mg m^{-3} in January 1999 and 2.6 mg m^{-3} in February 2001.

[13] To display the cross-shore CSAT structure we present a space-time plot from a section across the northern Patagonia shelf and shelf break (Figure 4, see Figure 1 for location). The inner shelf presents low CSAT values (<1.5 mg m^{-3}) throughout the record length. Though our section is located south of MS, two relative CSAT maxima (>1.5 mg m^{-3}) are apparent at the midshelf in April to May at 61°W and in August to October at 60–60.5°W

Table 1. Summary of CSAT Seasonal Cycle at Selected Patagonian Shelf Locations

Site	Position	Amplitude, mg m^{-3}	Month Max	Month Min
Midshelf	40.30°S 59.55°W	6.46	Oct	Mar
Valdés	42.85°S 62.97°W	3.11	Jan	Jun
Grande Bay	50.49°S 67.02°W	3.33	Jan	Aug
Shelf break	42.41°S 58.84°W	4.97	Nov	Jul
San Julián	49.17°S 66.40°W	8.43	Nov	Jul
Shelf break-S	50.14°S 60.51°S	9.21	Nov	Aug
Open shelf	45.04°S 62.97°W	2.6	Oct	Aug

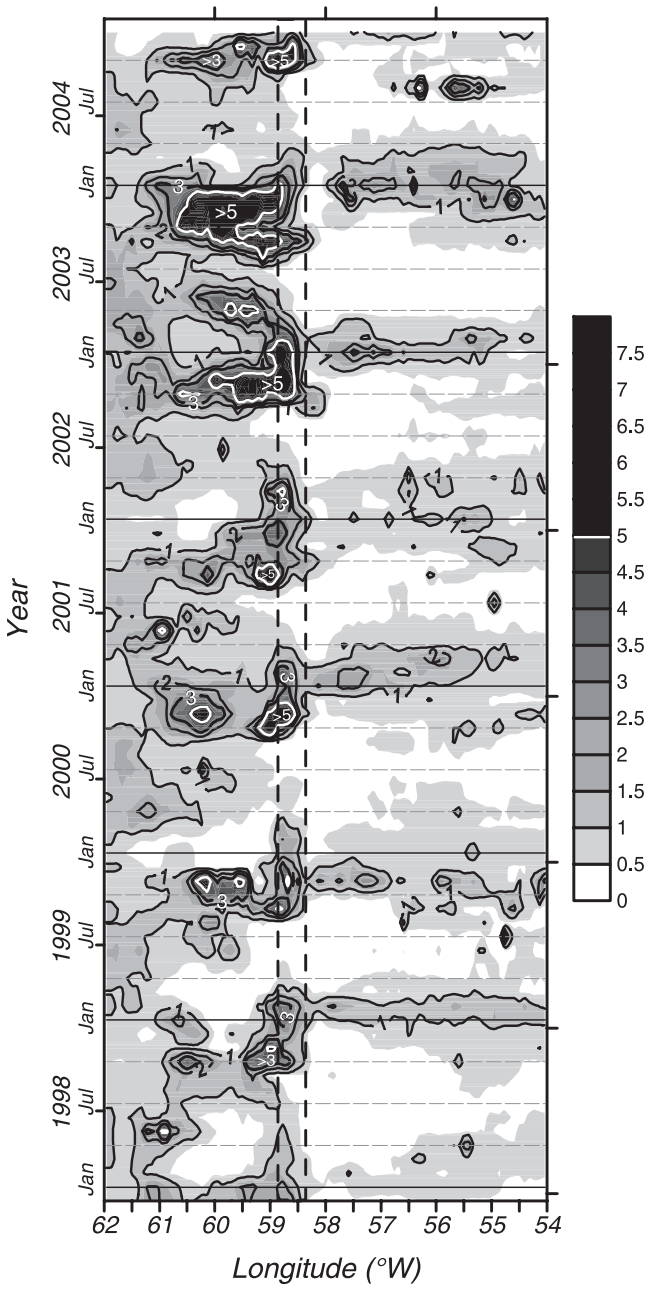

Figure 4. Space-time plot of SeaWiFS derived surface chl-*a* (mg m^{-3}) along the cross-shelf section shown in Figure 1. The dashed lines indicate the location of the 150 and 1000 m isobaths. The white contour is 5 mg m^{-3}.

(>2 mg m^{-3}). The September to March CSAT maxima at the shelf break present only slight displacements with time (Figure 4). In the early stages of the spring bloom the highest CSAT concentrations (>4 mg m^{-3}) are generally observed inshore of or at the 150 m isobath, while later on, in January to March, the bloom presents slightly lower CSAT concentrations and shifts offshore. After spring 2002 a significant CSAT increase (>5 mg m^{-3}) is observed in the midshelf and at the shelf break. The lowest CSAT concentrations are observed in a narrow band east of the PHCB, at the Malvinas Current axis. Further offshore moderate CSAT maxima (>1 mg m^{-3}) are observed in summer at the Brazil/Malvinas Confluence Zone (BMCZ, see Figures 1 and 2c and *Brandini et al.* [2000] and *Saraceno et al.* [2005]). In the austral summer of 2003–2004 the BMCZ presents relatively high CSAT concentrations (>1 mg m^{-3}) from December through March and, in contrast with previous years, values are higher than 2 mg m^{-3} (Figure 4).

3.3. Midshelf Front

[14] The spring (SON) midshelf bloom (>4 mg m^{-3}) is a narrow strip (~80 km wide) extending from 38 to 42°S (Figure 2b). This local maximum is embedded within the high CSAT region found north of 45°S. This feature can also be observed in the mean CSAT distribution for the 1998–2003 period presented by *Saraceno et al.* [2005, Figures 2 and 3]. We noted that CSAT at MS presents a distinct timing from other shelf regions (Figure 3a). On average, in spring CSAT at MS exceeds 3 mg m^{-3}, but in October 2002 it exceeded 10 mg m^{-3} (Figure 3b). Comparably high chl-*a* values are derived from in situ observations collected in September 1987 (>10 mg m^{-3}) and October 1988 (>7 mg m^{-3}) at 38°S, close to the northernmost reach of the midshelf front [*Carreto et al.*, 1995]. The in situ observations also show that the high chl-*a* off Cape Corrientes is associated to a surface temperature front separating well-mixed, nitrate-poor coastal waters from seasonally stratified midshelf waters. The mean austral spring distribution suggests that the midshelf high CSAT region is associated to a larger-scale feature extending southwestward about 450 km (Figure 2b). Notably, though there are suggestions of a weak surface temperature transition in the winter historical hydrographic data [*Martos and Piccolo*, 1988, Figure 4], there is only one recent report on this temperature front and no reports on the associated chl-*a* maximum in the literature. Synoptic hydrographic data collected in spring also show a moderate surface temperature front located offshore of the 50m isobath and, further offshore, a more intense bottom front induced by the deepening of the thermocline [*Lucas et al.*, 2005].

[15] To explore the relation between the high CSAT band observed at MS and surface temperature fronts we have computed the magnitude of the spring (SON) surface temperature gradient based on the analysis of 13 years (1985–1997) of satellite data [*Casey and Cornillon*, 1999, 2001]. Figure 5 reveals a moderate SST gradient band (~0.02°C km^{-1}) close to the 80 m isobath and also closely following the high CSAT band observed in spring at midshelf. The low CSAT region off El Rincón is located inshore of the thermal front. The SST front is also apparent in the recent analysis of *Saraceno et al.* [2004, Figure 3]. The similarity of these spatial patterns suggests that along most of its extension the high CSAT band is associated to temperature fronts separating coastal and midshelf waters in spring, as observed off Cape Corrientes [*Carreto et al.*, 1995]. Though the satellite derived SST data reveal that the surface temperature front is present throughout the year (not shown) the associated CSAT maximum presents a strong seasonality.

3.4. Patagonia Tidal Fronts

[16] In fall, winter, and spring a CSAT maximum around Valdés Peninsula (1.5–2 mg m^{-3}) is observed across the mouth of San Matías Gulf (Figure 2). Regional numerical

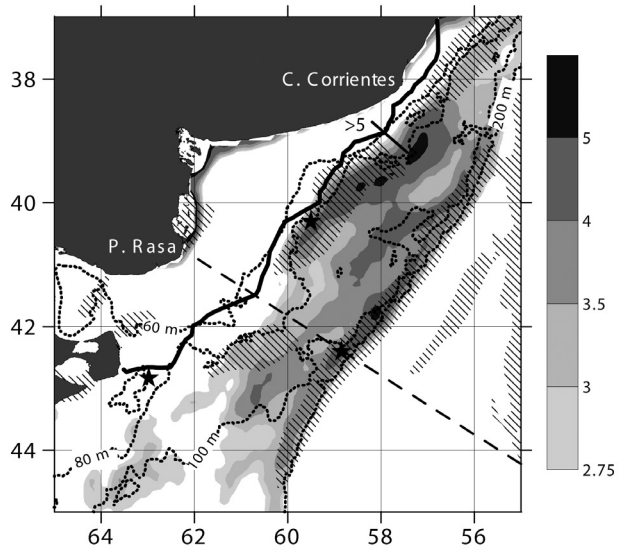

Figure 5. Austral spring (SON) SeaWiFS derived surface chl-*a* (mg m^{-3}) distribution in the region of the midshelf front (gray shading). The hatched area marks the regions of high sea surface temperature gradient ($\sim$0.014°C km^{-1}) in spring and the heavy line is the Simpson stability parameter 60 J m^{-3} (adapted from *Lucas et al.* [2005]). The dashed line indicates the location of the space-time plot shown in Figure 4. Dotted lines indicate the 60, 80, 100, and 200 m isobaths.

simulations show that this is a region of high tidal dissipation and enhanced vertical mixing [*Glorioso and Flather*, 1995; *Palma et al.*, 2004]. The spring surface chl-*a* increase in the well mixed region is confirmed by early in situ observations [*Proyecto de Desarrollo Pesquero*, 1971]. In summer, in addition to this relatively high CSAT region (>1.3 mg m^{-3}), an elongated CSAT maximum band (>2 mg m^{-3}) develops east and southeast of Valdés Peninsula (Figures 2c and 6). In austral spring and summer the feature extends southwestward approaching the coast off Cape Dos Bahias (Figures 2b and 2c). The CSAT maximum location closely follows the transition between the homogeneous coastal zone and the stratified midshelf [*Sabatini and Martos*, 2002]. The time series at VP is located east of the Peninsula and presents large seasonal CSAT amplitude with maxima in January (CSAT > 2.5 mg m^{-3}, Figure 6) and February. Though there is large interannual variability at VP (Figure 3b) this high CSAT band is observed every summer at the same location, offshore of the high tidal dissipation band (Figure 6). A region of low surface temperature (<17°C) surrounds Valdés Peninsula and extends southward along the coast (Figure 6). The temperature pattern is similar to the observations reported by *Glorioso* [1987], who also referred to the 17°C isotherm as indicative of a sea surface temperature front in January 1983. The location of the tidal front is also depicted by the critical Simpson parameter of vertical stability (Φ_c) within the range 40–50 J m^{-3}, derived from spring-summer historical hydrographic data [*Sabatini and Martos*, 2002; *Bianchi et al.*, 2005]. Off Valdés Peninsula Φ_c is also located close to the 17°C isotherm. The mean January high CSAT band (>2.5 mg m^{-3}) extends along this same region and offshore of the high SST gradient that surrounds the surface temperature minimum (Figure 6). These observations confirm that the Valdés high CSAT band in summer is related to the combination of the strong Patagonian shelf tidal currents with the bottom topography, as proposed by *Glorioso* [1987].

[17] Additional CSAT maxima are observed in the near-coastal and midshelf regions of southern Patagonia. In summer these maxima are located north of 52°S and extend northward along a broad band to about 46°S (Figure 7). South of 51°S and east of 65°W the Patagonia shelf presents weak stratification even in summer [*Sabatini et al.*, 2004; *Bianchi et al.*, 2005]. In March a moderate surface temperature front extending northeastward from the coast at 51°S separates the stratified northern zone from the well-mixed southern zone [*Sabatini et al.*, 2004]. Inspection of the Pathfinder SST climatology (1985–1997) confirms the existence of the front, here referred to as South Patagonia Front (SPF), from October through April (not shown). Though the SPF is of moderate intensity, as pointed out by *Sabatini et al.* [2004], it is unlikely that the southward

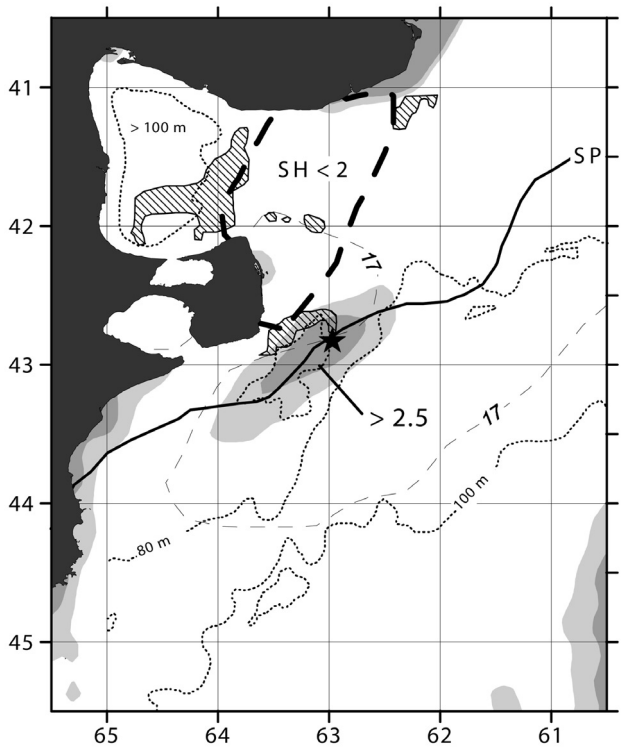

Figure 6. Mean January SeaWiFS derived surface chl-*a* (mg m^{-3}) distribution in the region of Valdés Peninsula (gray shading: light gray >2 mg m^{-3}, dark gray >2.5 mg m^{-3}). The hatched areas mark the regions of high sea surface temperature gradient in January (>0.25°C km^{-1}, adapted from *Bava et al.* [2002]). The heavy dashed line encloses the low Simpson-Hunter parameter region (SH < 2, adapted from *Palma et al.* [2004]). The heavy solid line is the Simpson Parameter critical value (<50 J m^{-3}, adapted from *Bianchi et al.* [2005]) and the thin dashed line is the mean position of the 17°C isotherm in January. Dotted lines indicate the 80 and 100 m isobaths.

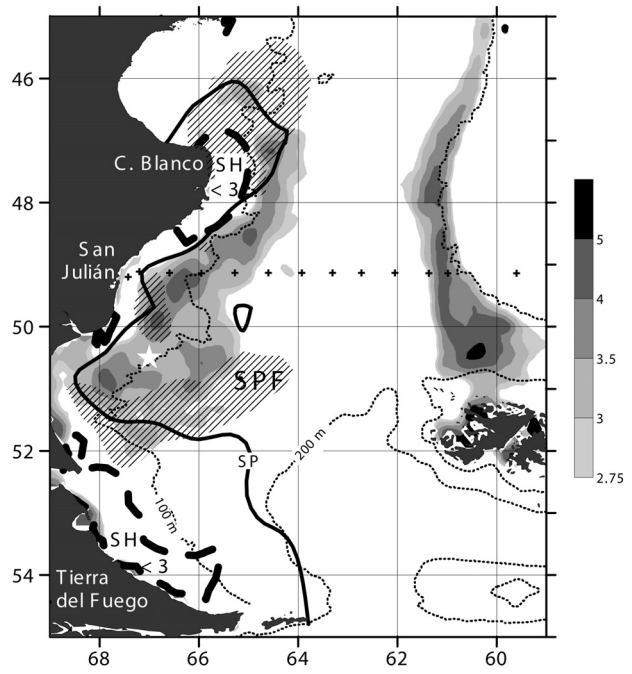

Figure 7. Mean summer (DJF) SeaWiFS derived surface chl-*a* (mg m^{-3}) distribution off southern Patagonia (gray shading). The hatched area marks the region of high sea surface temperature gradient (>0.01°C km^{-1}) in January. SPF indicates the Southern Patagonia Front. The heavy dashed line encloses the low Simpson-Hunter parameter region (SH < 3, adapted from *Palma et al.* [2004]). The heavy line is the Simpson Parameter critical value (<50 J m^{-3}, adapted from *Bianchi et al.* [2005]). The white star marks the location of the time series shown in Figure 3 and (cross) the location of the hydrographic section presented in Figure 8. Dotted lines indicate the 100 and 200 m isobaths.

decrease in heat flux from the atmosphere can account for this feature. As its intensity decreases, the offshore extension of the SPF presents a slight northward shift in April and May. The southern Patagonia CSAT summer blooms do not extend southward of the SPF (Figures 2 and 7).

[18] The cross-shelf frontal structure in southern Patagonia is depicted by a temperature section composite from late January to early February, occupied at 49°S (Figure 8b). The section reveals a narrow (~30 km) near-coastal band of relatively cold (~11.5°C) well mixed waters. Further offshore a sharp seasonal thermocline develops. The summer (DJF) cross shelf CSAT distribution presents a relative maximum (>5 mg m^{-3}) at ~90 km from shore and decreases throughout the midshelf (Figure 8a). CSAT also presents a relative maximum at the shelf break (4.5 mg m^{-3}). At the two stations closer to shore the Simpson parameter is lower than 50 J m^{-3}, while at station 37, located 75 km from the coast the Simpson parameter increases to 125 J m^{-3}. Thus the well-mixed waters extend northward along the coast and appear to form a continuous band reaching the strong tidal mixing domain off Cabo Blanco (Figure 7).

3.5. Patagonia Shelf Break

[19] In early spring CSAT increases simultaneously over the shelf break and over the mid and outer shelves to values higher than 5 mg m^{-3}. In contrast, in summer the PHCB presents a well defined maximum (Figure 4) that extends along the entire shelf break from 37 to 51°S (Figure 2c).

[20] Hydrographic data from September 1997 extending from the outer shelf to the open ocean off northern Patagonia illustrate the cross-shelf property structure in the vicinity of the PHCB and its possible relation to the increased CSAT observed at the shelf break (Figure 9). The transition between shelf and Malvinas Current waters forms a cold upper layer band bounded by outcropping temperature, density and nitrate isopleths. In summer the western isotherm outcrop thus creates a relatively intense surface temperature front [see *Saraceno et al.*, 2004]. Since throughout the year the cross-front structure always depicts a well defined salinity contrast, the front location is well represented by the surface outcrop of the 33.9 isohaline (shown in Figure 1). A relative temperature minimum (<5.5°C) and density maximum (σ_T > 26.8 kg m^{-3}) is observed at CTD station 19. Surface salinity at station 19 is >34.1, this is the core of the low SST that characterizes the northward flowing Malvinas Current. West of the low temperature core there is a moderate temperature increase (to 7°C at station 14) and a sharp salinity decrease (S < 33.8). In early austral spring nitrates are relatively high (>10 μmol kg^{-1}) along the entire cross-shelf section, but a local surface maximum (>15 μmol kg^{-1}) is observed at stations 16–18 (Figure 9c). Data from two hydrographic sections collected in March 1994 and 1996 (not shown) present a similar thermohaline structure across the shelf break, a strong surface to bottom cross-shelf salinity front with a salinity increase from 33.9 to 34.1 in 90 km. The salinity front and nitrate maxima are located at or inshore of the surface temperature minimum and density maximum.

[21] Though due to cloud cover satellite color data corresponding to September 1997 were of limited use, a high resolution image from 25 September was used for comparison with the hydrographic data collected 10 days

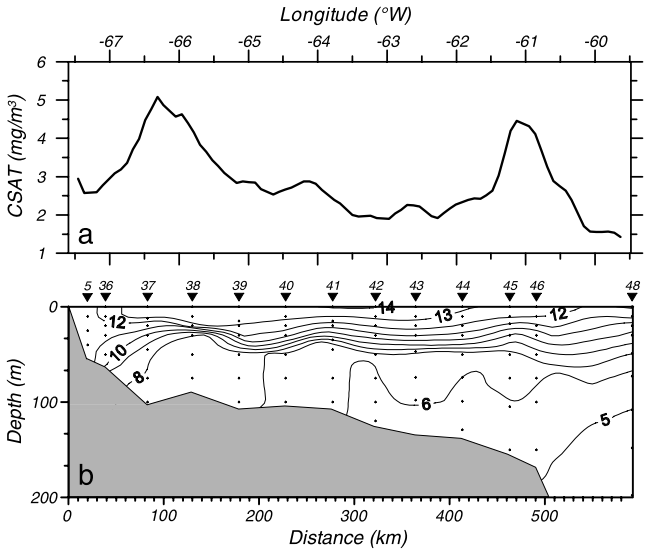

Figure 8. (a) Austral summer (DJF) surface chl-*a* (mg m^{-3}) derived from SeaWiFS climatology and (b) late January to early February cross-shelf temperature section (°C) off Grande Bay (see Figure 7 for location).

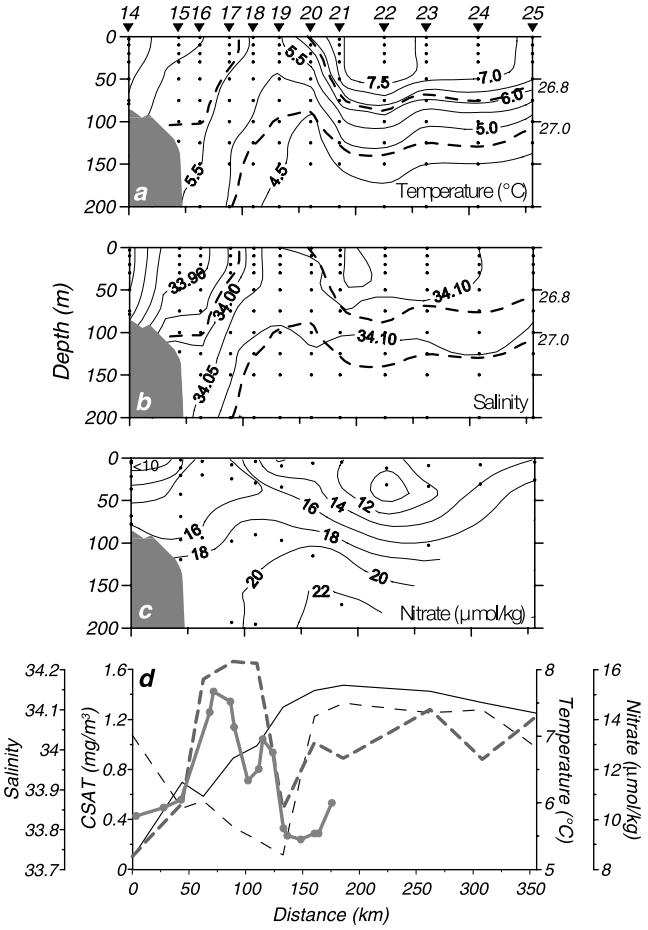

Figure 9. (a) Temperature (°C), (b) salinity, and (c) nitrate (μmol Kg^{-1}) on a hydrographic section across the Patagonia shelf break collected in September 1997 (see Figure 1 for location). The dashed lines in Figures 9a and 9b are the 26.8 and 27 kg m^{-3} isopycnals (sigma-T). (d) The surface temperature (°C, thin dashed line), salinity (thin solid line), nitrate (μmol kg^{-1}, heavy dashed line), and SeaWiFS chl-*a* (mg m^{-3}, heavy solid line) from 25 September 1997 along the same line.

earlier. CSAT data shows that the PHCB in late September 1997 was colocated with the high surface nutrient and temperature and salinity gradient maxima, offshore of the 200 m isobath. Such location is just offshore of the climatological mean position of the PHCB in spring (Figure 2b). SeaWiFS data reveal a similar offshore displacement of the PHCB in September 2002 (not shown).

4. Discussion

[22] High biological production is usually related to the occurrence of shelf fronts [*Simpson*, 1981]. The midshelf front separates well-mixed nearshore waters from stratified waters further offshore. Since there is no evidence of strong tidal mixing in this region [*Glorioso and Flather*, 1995; *Palma et al.*, 2004], the wind is likely to provide a substantial part of the energy required to vertically mix the water column in the near coastal waters. This is in contrast with other shelf sea fronts generated by enhanced vertical mixing associated to interaction of strong tidal flows with the ocean bottom, such as at some near-coastal locations off Patagonia. If wind energy is a significant mixing source, some variability of frontal location in response to variations of wind intensity is expected. Off Cape Corrientes the location of the SST front and the high CSAT band appear to follow closely the transition between two midshelf bottom terraces located at 25–30 m and 80 m [see *Parker et al.*, 1997]. This is in agreement with the in situ observations recently reported by *Lucas et al.* [2005]. Presumably, large changes in wind-induced vertical mixing would be required to displace the front away from the terrace location. The SST gradient monthly means, however, suggest that the location of the SST front is more variable south of 41°S. Since the bottom slope is significantly less steep than farther north [see *Parker et al.*, 1997] the front location south of 41°S is possibly more sensitive to variations in wind stress. Historical hydrographic data reveal that during the warm season the transition from coastal well-mixed waters to stratified midshelf waters is weaker between 39 and 41°S than further north and south [*Lucas et al.*, 2005, Figure 8a]. Thus the midshelf front weakens and its location is more variable as the bottom slope decreases.

[23] South of 40°S the most outstanding inner shelf CSAT features are the blooms observed at the Valdés Peninsula, San Jorge Gulf, and Grande Bay-San Julián. In situ, satellite SST observations and numerical models show that all these near-coastal sites are close to regions of high tidal energy dissipation where the water column is vertically mixed throughout the year [*Carreto et al.*, 1986; *Glorioso*, 1987; *Glorioso and Simpson*, 1994; *Glorioso and Flather*, 1995; *Sabatini and Martos*, 2002; *Palma et al.*, 2004; *Bogazzi et al.*, 2005]. The Patagonia tidal fronts are important for their influence on the distribution of several species [see *Acha et al.*, 2004 and references therein], including toxic blooms [*Carreto et al.*, 1986]. In summer, when midshelf waters are strongly stratified, a surface temperature front develops at the seaward edge of these regions [*Glorioso*, 1987; *Glorioso and Simpson*, 1994; *Palma et al.*, 2004]. The correspondence between regions of large tidal dissipation and high CSAT observed in summer strongly suggests that tidal induced mixing plays a major role in the redistribution of nutrients and in maintaining the relatively high CSAT in these near-coastal sites.

[24] Along its northward extension the high CSAT band of southern Patagonia is located about 30–50 km from the coast (with concentrations > 2.7mg m^{-3}), while the CSAT maximum (>4 mg m^{-3}) is located on average 85 km from the coast (Figure 7). Historical hydrographic data present a transition in stratification, between a well-mixed near coastal band and stratified waters further offshore (e.g., *Bianchi et al.* [2005] and Figure 8). The recent analysis of *Sabatini et al.* [2004] suggested that stratified waters are found everywhere north of 51°S (their Figure 5). Inspection of the data used in this study (their Figure 1) shows that north of 51°S no stations were occupied inshore of the 50m isobath, thus probably missing the narrow, well mixed coastal band, which is evident in the historical data. Recent data collected off GB in March confirm the existence of a narrow, well-mixed band extending northward along the coast (R. Reta, personal communication, 2005). In summer

the high CSAT band in southern Patagonia is observed north of the SPF, and between 51 and 46°S, along a band located just offshore of the narrow quasi homogeneous waters found along the coast (Figure 7).

[25] East of Valdés Peninsula, the Valdés tidal front presents high nutrient concentrations on the stratified side of the front [*Carreto et al.*, 1986; *Carreto and Benavides*, 1989]. In contrast, cross shelf sections occupied off Cape Corrientes [*Carreto et al.*, 1995] throughout the year reveal warm, low nitrate concentrations in the inshore side of the midshelf front. Similarly, at the mouth of San Matías Gulf, which presents relatively high CSAT during most of the year (Figure 2), the mixed side of the front is warm and nutrient poor [see *Carreto et al.*, 1986, Figures 5 and 6]. These observations suggest that cross front fluxes are not a driving mechanism for sustaining the high phytoplankton biomass inferred from the CSAT distribution at these locations.

[26] Theory predicts that a three layer residual circulation establishes on the stratified side of the front, with onshore flow in the near-surface and near-bottom layers and offshore flow at the pycnocline [*Bo Pedersen*, 1994]. Cross-shore flows within the lower layer can therefore supply new nutrients to the thermocline layer near the front, leading to the development of chl-*a* maxima on the stratified side of the front. In situ observations of near frontal chl-*a* maxima at thermocline level from several locations off Argentina [*Carreto et al.*, 1986; *Carreto et al.*, 1995] and elsewhere [see *Bo Pedersen*, 1994, and references therein] seem to confirm this theoretical prediction. The data also show that the chl-*a* maximum frequently extends to the surface layer near the frontal location, which would contribute to the formation of along-front high CSAT bands reported in this study (Figures 5–7).

[27] The most intense surface temperature gradient across the shelf break front off Patagonia is found in the austral summer and fall, and the weakest gradients in winter and spring [*Saraceno et al.*, 2004]. This moderate cross front surface temperature gradient ($\sim$0.11°C km^{-1} north of 44°S) is trapped to the bottom topography closely following the shelf break. In summer CSAT presents a sharp eastward decrease across the shelf break. In contrast, during the austral winter (May to August) CSAT decreases sharply (0.6 ± 0.2 mg m^{-3}) throughout the region (Figure 2a). The low CSAT concentrations in winter are probably due to the reduced stratification [see *Rivas and Piola*, 2002] and solar radiation. In winter strong vertical mixing leads to relatively high nutrient concentrations throughout the water column [e.g., *Brandhorst and Castello*, 1971; *Carreto et al.*, 1995]. By early summer, north of 45°S, nutrient concentrations are too low to sustain further phytoplankton development away from frontal regions [*Carreto et al.*, 1995]. However, along the narrow PHCB enhanced vertical mixing or cross front nutrient fluxes are required to sustain the high phytoplankton biomass suggested by the CSAT distributions in summer.

[28] Earlier numerical models predict that an alongshelf flow leads to the formation of a bottom trapped front at the shelf break [*Chapman and Lentz*, 1994] with convergent flow in the bottom boundary layer and upwelling along the front, which intensifies with increased vertical stratification [*Gawarkiewicz and Chapman*, 1992]. Recent numerical simulations, however, suggest that bottom friction associated to the presence of a strong slope current, such as the Malvinas Current, creates along-shelf pressure gradients and lead to robust upwelling at the shelf break. This upwelling regime is controlled by the magnitude of the slope flow and not by the shelf circulation (R. Matano and E. Palma, personal communication, 2005). The termination of the high CSAT band close to the separation of the Malvinas Current from the slope appears to confirm this theoretical result. Observations of weak ($\sim$0.01–0.02 m s^{-1}) and persistent near-bottom cross-shore circulations and relatively intense isopycnal upwelling (up to 17 m day^{-1}) derived from near bottom dye release and lagrangean experiments conducted in the shelf break front in the northwest North Atlantic have confirmed the model predictions [*Houghton*, 1997; *Houghton and Visbeck*, 1998; *Barth et al.*, 2004]. The cross shelf hydrographic structure at the Patagonian shelf break presents some similarities with the transition between the relatively cold-fresh shelf waters and the warm-salty Slope Water in the western North Atlantic: a persistent, surface-to-bottom front intersecting the sea bottom near the shelf break and the surface some tens of km offshore. Also as in the Patagonia shelf break, observations in the western North Atlantic reveal high surface chlorophyll concentrations along the front [e.g., *Marra et al.*, 1990]. Off Patagonia the convergent bottom flows derived from the shelf lower layer and from the subantarctic waters found further offshore, could carry nutrient rich waters to the shelf break. The subsequent upwelling at the shelf break would lead to the development of the high CSAT band along the shelf break. The PHCB terminates near the high SST gradient region associated to the Brazil/Malvinas Confluence ($\sim$37–39°S) [*Saraceno et al.*, 2005], where the Malvinas Current veers offshore [*Podestá*, 1997]. Therefore the combination of nutrient-rich subantarctic waters, bottom boundary layer convergence, and the vertical stratification over the outer shelf appear to be relevant processes inducing the extensive high surface chl-*a* band observed along the Patagonian shelf break.

5. Conclusions

[29] The analysis of 7 years of ocean-color data (1998–2004) from SeaWiFS reveals the largest CSAT seasonal variability (>4 mg m^{-3}) is located over the Patagonian continental shelf. Throughout the year the region presents relatively high CSAT concentrations relative to the open ocean. North of about 45°S CSAT blooms initiate in early austral spring (September and October) while south of 45°S blooms begin in late spring to early summer (November to January). The seasonal CSAT cycle in the northern midshelf region presents the lowest concentrations in late austral summer (February and March) and a well-defined secondary maximum in early winter (June). All high CSAT regions present substantial interannual variations, but the bloom locations are remarkably stable because they are associated to bottom trapped fronts. The CSAT maxima are found along a 80 km wide midshelf strip extending from 38 to 42°S; over a $\sim$50 km wide, 1500 km strip extending along the shelf break from 37 to 51°S and in two inner shelf regions located off Valdés Peninsula and along a band extending between Cape Blanco and Grande Bay off southern Patagonia. Though CSAT concentrations over the

midshelf sharply decrease in late spring, the shelf break maximum persists throughout the summer, indicating an effective nutrient supply to the upper layer throughout the warm season. The high CSAT concentrations and interannual variability observed over the southwest Atlantic continental shelf relative to the deep adjacent ocean revealed by the SeaWiFS data may explain why the region presents one of the highest CSAT trends estimated in the World Ocean [*Gregg et al.*, 2005]. The recent analysis of *Saraceno et al.* [2005] suggests that the recent CSAT increase observed in the southwest South Atlantic may be related to the enhanced northerly winds in austral spring of 2002–2003, compared to 2001–2002. The substantial interannual variability, which arises primarily over these highly productive regions, suggests that trend estimates based on the relatively short record length available should be interpreted with caution. All the high CSAT locations are closely associated with frontal systems, suggesting that frontal enhanced vertical circulations play a central role in supplying nutrients to the upper layer. A recent study has shown that the Patagonian tidal fronts, which bound the near coastal high CSAT regions, are interfaces separating regions of CO_2 flux to the atmosphere, on the near-coastal well-mixed side, from stratified regions where the CO_2 flux is into the ocean [*Bianchi et al.*, 2005]. The results presented here suggest that enhanced vertical circulations at these frontal systems also play a significant role in shaping the patterns and variability of the regional chl-*a* distributions.

[30] **Acknowledgments.** This research was funded by the Inter-American Institute for Global Change Reasearch grant CRN-61 and Fundación Antorchas grant 13900-13. The SeaWiFS Project (Code 970.2) and the Distributed Active Archive Center (Code 902) at NASA Goddard Space Flight Center produced and distributed the satellite data. Additional satellite data from the HRPT stations were provided by Comisión Nacional de Actividades Espaciales (Argentina) and Fundaçao Universidade Federal do Rio Grande (Brazil). Comments from A. Bianchi, R. Reta, M. Saraceno, and the anonymous reviewers are greatly acknowledged. L. Bianucci, N. Martinez, and U. Zajaczkovski assisted in the data processing.

References

Acha, E. M., H. W. Mianzan, R. A. Guerrero, M. Favero, and J. Bava (2004), Marine fronts at the continental shelves of austral South America, physical and ecological processes, *J. Mar. Syst.*, *44*, 83–105.

Barth, J. A., D. Hebert, A. C. Dale, and D. S. Ullman (2004), Direct observations of along-isopycnal upwelling and diapycnal velocity at a shelfbreak front, *J. Phys. Oceanogr.*, *34*, 543–565.

Bava, J., D. A. Gagliardini, A. I. Dogliotti, and C. A. Lasta (2002), Annual distribution and variability of remotely sensed sea surface temperature fronts in the southwestern Atlantic Ocean, paper presented at 29th International Symposium on Remote Sensing of the Environment, Int. Soc. for Remote Sens. of the Environ., Buenos Aires, Argentina, 8–12 April.

Bertolotti, M. I., N. E. Brunetti, J. I. Carreto, L. B. Prenski, and R. Sánchez (1996), Influence of shelf-break fronts on shellfish and fish stocks off Argentina, *C.M. 1996/S*, 41 pp., Int. Council for the Explor. of the Sea, Copenhagen.

Bianchi, A. A., L. Bianucci, A. R. Piola, D. Ruiz Pino, I. Schloss, A. Poisson, and C. F. Balestrini (2005), Vertical stratification and air-sea CO_2 fluxes in the Patagonian shelf, *J. Geophys. Res.*, *110*, C07003, doi:10.1029/2004JC002488.

Bogazzi, E., A. Baldoni, A. Rivas, P. Martos, R. Reta, J. M. Orensanz, M. Lasta, P. Dell'Arciprete, and F. Werner (2005), Spatial correspondence between areas of concentration of Patagonian scallop (*Zygochlamys patagonica*) and frontal systems in the southwestern Atlantic, *Fish. Oceanogr.*, *14*, 359–376.

Bo Pedersen, F. (1994), The oceanographic and biological tidal cycle succession in shallow sea fronts in the North Sea and the English Channel, *Est. Coast. Shelf Sci.*, *38*, 249–269.

Brandhorst, W., and J. P. Castello (1971), Evaluación de los recursos de anchoita (*Engraulis Anchoita*) frente a la Argentina y Uruguay I: Las condiciones oceanográficas, sinopsis del conocimiento actual sobre la anchoita y el plan para su evaluación, *Proy. Des. Pesq. Ser. Inf. Tec. 29*, 63 pp.

Brandini, F. P., D. Boltovskoy, A. R. Piola, S. Kocmur, R. Rottgers, P. C. Abreu, and R. Mendes Lopes (2000), Multiannual trends in fronts and distribution of nutrients and chlorophyll in the southwestern Atlantic (30–62°S), *Deep Sea Res. I*, *47*, 1015–1033.

Brown, C. W., and G. P. Podestá (1997), Remote sensing of coccolithophore blooms in the Southwestern Atlantic Ocean, *Remote Sens. Environ.*, *60*, 83–91.

Carreto, J. I., and H. R. Benavides (1989), Phytoplankton, in *Second Workshop on Sardine/Anchovy Recruitment Project (SARP) in the Southwest Atlantic*, *Workshop Rep. 65*, Intergov. Ocean. Comm., Montevideo, Uruguay, 21–23 August.

Carreto, J. I., H. R. Benavides, R. M. Negri, and P. D. Glorioso (1986), Toxic red-tide in the Argentine Sea. Phytoplankton distribution and survival of the toxic dinoflagellate *Gonyaulax excavate* in a frontal area, *J. Plankton Res.*, *8*, 15–28.

Carreto, J. I., V. A. Lutz, M. O. Carignan, A. D. C. Colleoni, and S. G. D. Marcos (1995), Hydrography and chlorophyll-a in a transect from the coast to the shelf-break in the Argentinean Sea, *Cont. Shelf Res.*, *15*, 315–336.

Casey, K. S., and P. Cornillon (1999), A comparison of satellite and in situ based sea surface temperature climatologies, *J. Clim.*, *12*, 1848–1863.

Casey, K. S., and P. Cornillon (2001), Global and regional sea surface temperature trends, *J. Clim.*, *14*, 3801–3818.

Chapman, D. C., and S. J. Lentz (1994), Trapping of a coastal density front by the bottom boundary layer, *J. Phys. Oceanogr.*, *24*, 1464–1479.

Dandonneau, Y., P.-Y. Deschamps, J.-M. Nicolas, H. Loisel, J. Blanchot, Y. Montel, F. Thieuleux, and G. Bécu (2004), Seasonal and interannual variability of ocean color and composition of phytoplankton communities in the North Atlantic, equatorial Pacific and South Pacific, *Deep Sea Res., Part II*, *51*(1–3), 303–318.

Feldman, G. C., and C. R. McClain (2005), SeaWiFS chlorophyll trends (4.0_4.1), in *Ocean Color Web*, edited by N. Kuring et al., NASA Goddard Space Flight Center, Greenbelt, Md. (Available at http://oceancolor.gsfc.nasa.gov/REPROCESSING/SeaWiFS/R4.1/)

Food and Agricultural Organization (FAO) (1994), World review of highly migratory and straddling stocks, *Fish. Tech. Pap. 337*, Rome.

Forbes, M. C., and Z. Garraffo (1988), A note on the mean seasonal transport on the Argentinian Shelf, *J. Geophys. Res.*, *93*, 2311–2319.

Framiñan, M. B., and O. B. Brown (1996), Study of the Río de la Plata turbidity front, Part I: Spatial and temporal distribution, *Cont. Shelf Res.*, *16*, 1259–1282.

Garcia, C. A. E., Y. V. B. Sarma, M. M. Mata, and V. M. T. Garcia (2004), Chlorophyll variability and eddies in the Brazil-Malvinas Confluence region, *Deep Sea Res.*, *51*(1–3), 159–172.

Garcia, C. A. E., V. M. T. Garcia, and C. R. McClain (2005), Evaluation of SeaWiFS chlorophyll algorithms in the Southwestern Atlantic and Southern Oceans, *Remote Sens. Environ.*, *95*, 125–137.

Gawarkiewicz, G., and D. C. Chapman (1992), The role of stratification in the formation and maintenance of shelf-break fronts, *J. Phys. Oceanogr.*, *22*, 753–772.

Glorioso, P. D. (1987), Temperature distribution related to shelf-sea fronts on the Patagonian shelf, *Cont. Shelf Res.*, *7*, 27–34.

Glorioso, P. D., and R. A. Flather (1995), A barotropic model of the currents off SE South America, *J. Geophys. Res.*, *100*, 13,427–13,440.

Glorioso, P. D., and J. H. Simpson (1994), Numerical modeling of the M2 tide on the northern patagonian shelf, *Cont. Shelf Res.*, *14*, 267–278.

Gregg, W. W., and M. E. Conkright (2002), Decadal changes in global ocean chlorophyll, *Geophys. Res. Lett.*, *29*(15), 1730, doi:10.1029/2002GL014689.

Gregg, W. W., N. W. Casey, and C. R. McClain (2005), Recent trends in global ocean chlorophyll, *Geophys. Res. Lett.*, *32*, L03606, doi:10.1029/2004GL021808.

Guerrero, R. A., and A. R. Piola (1997), Masas de agua en la Plataforma Continental, in *El Mar Argentino y sus Recursos Pesqueros*, vol. 1, edited by E. Boschi, pp. 107–118, Inst. Nac. de Invest. y Desarrollo Pesquero, Mar del Plata, Argentina.

Houghton, R. W. (1997), Lagrangian flow at the foot of a shelfbreak front using a dye tracer injected into the bottom boundary layer, *Geophys. Res. Lett.*, *24*, 2035–2038.

Houghton, R. W., and M. Visbeck (1998), Upwelling and convergence in the Middle Atlantic Bight shelfbreak front, *Geophys. Res. Lett.*, *25*, 2765–2768.

Huret, M., I. Dadou, F. Dumas, P. Lazure, and V. Garçon (2005), Coupling physical and biogeochemical processes in the Río de la Plata plume, *Cont. Shelf Res.*, *25*, 629–653.

Longhurst, A. (1998), *Ecological Geography of the Sea*, 398 pp., Elsevier, New York.

Lucas, A. J., R. A. Guerrero, M. W. Mianzan, E. M. Acha, and C. A. Lasta (2005), Coastal oceanographic regimes of the Northern Argentine Continental Shelf (34–43°S), *Estuar. Coast. Shelf Sci.*, *65*, 405–420, doi:10.1016/j.ecss.2005.06.015.

Lutz, V. A., A. Subramaniam, R. M. Negri, R. I. Silva, and J. I. Carreto (2006), Annual variation in bio-optical properties at the EPEA coastal Station (Argentina), *Cont. Shelf Res.*, in press.

Marra, J., R. W. Houghton, and C. Garside (1990), Phytoplankton growth at the shelf-break front in the Middle Atlantic Bight, *J. Mar. Res.*, *48*(4), 851–868.

Martos, P., and M. C. Piccolo (1988), Hydrography of the Argentine Continental shelf between 38° and 42°S, *Cont. Shelf Res.*, *8*, 1043–1056.

Mouzo, F. H. (1982), Geología marina y fluvial, in *Historia Marítima Argentina*, vol. 1, pp. 47–117, Armada Argentina, Dep. Estudios Históricos Navales, Cuántica Editora S.A., Buenos Aires, Argentina.

Negri, R. M., J. I. Carreto, H. R. Benavides, R. Akselman, and V. A. Lutz (1992), An unusual bloom of *Gyrodinium* cf. *aureolum* in the Argentine sea: Community structure and conditioning factors, *J. Plankton Res.*, *14*(2), 261–269.

O'Reilly, J. E., S. Maritorena, G. Mitchell, D. A. Siegel, K. L. Carder, S. A. Garver, M. Kahru, and C. McClain (1998), Ocean color chlorophyll algorithms for SeaWiFS, *J. Geophys. Res.*, *103*, 24,937–24,953.

Palma, E. D., R. P. Matano, and A. R. Piola (2004), Three dimensional barotropic response of the southwestern Atlantic shelf circulation to tidal and wind forcing, *J. Geophys. Res.*, *109*, C08014, doi:10.1029/2004JC002315.

Parker, G., C. M. Paterlini, and R. A. Violante (1997), El Fondo Marino, in *El Mar Argentino y sus Recursos Pesqueros*, vol. 1, edited by E. Boschi, pp. 65–87, Inst. Nac. de Investigación y Desarrollo Pesquero, Mar del Plata, Argentina.

Patt, F. S., et al. (2003), Algorithm updates for the fourth SeaWiFS data reprocessing, *NASA Tech. Memo 2003–206892 22*, 74 pp., edited by S. B. Hooker and E. R. Firestone, NASA Goddard Space Flight Center, Greenbelt, Md.

Piola, A. R., and A. L. Gordon (1989), Intermediate waters in the southwest South Atlantic, *Deep Sea Res.*, *36*, 1–16.

Piola, A. R., and A. L. Rivas (1997), Corrientes en la Plataforma Continental, in *El Mar Argentino y sus Recursos Pesqueros*, vol. 1, edited by E. Boschi, pp. 119–132, Inst, Nac. de Investigación y Desarrollo Pesquero, Mar del Plata, Argentina.

Piola, A. R., and S. I. Romero (2004), Analysis of space-time variability of the Plata River Plume, *Gayana*, *68*, 482–486.

Podestá, G. P. (1988), Migratory pattern of Argentine hake (Merluccius hubbsi) and oceanic processes in the southwestern Atlantic Ocean, *Fish. Bull.*, *88*, 167–177.

Podestá, G. P. (1997), Utilización de datos satelitarios en investigaciones oceanográficas y pesqueras en el Océano Atlántico Sudoccidental, in *El Mar Argentino y sus Recursos Pesqueros*, vol. 1, edited by E. Boschi, pp. 195–222, Inst. Nac. de Investigación y Desarrollo Pesquero, Mar del Plata, Argentina.

Proyecto de Desarrollo Pesquero (1971), Datos y resultados de las campañas Pesquería, in *Pesquería X*, edited by S. F. Villanueva, Mar del Plata, Argentina.

Rivas, A. L. (1997), Current meter observations in the Argentine Continental Shelf, *Cont. Shelf Res.*, *17*, 391–406.

Rivas, A. L., and A. R. Piola (2002), Vertical stratification at the shelf off northern Patagonia, *Cont. Shelf Res.*, *22*, 1549–1558.

Rodhouse, P. G., C. D. Elvidge, and P. N. Trathan (2001), Remote sensing of the global light-fishing fleet: an analysis of interactions with oceanography, other fisheries and predators, *Adv. Mar. Biol.*, *39*, 261–303.

Sabatini, M., and P. Martos (2002), Mesozooplankton features in a frontal area off northern Patagonia (Argentina) during spring 1995 and 1998, *Sci. Mar.*, *63*, 215–232.

Sabatini, M., R. Reta, and R. Matano (2004), Circulation and zooplankton biomass distribution over the southern Patagonian shelf during late summer, *Cont. Shelf Res.*, *24*, 1359–1373.

Sánchez, R., and J. D. Ciechomski (1995), Spawning and nursery grounds of pelagic fish species in the sea-shelf off Argentina and adjacent areas, *Sci. Mar.*, *59*, 455–478.

Saraceno, M., C. Provost, A. R. Piola, A. Gagliardini, and J. Bava (2004), Brazil Malvinas Frontal System as seen from nine years of advanced very high resolution radiometer data, *J. Geophys. Res.*, *109*, C05027, doi:10.1029/2003JC002127.

Saraceno, M., C. Provost, and A. R. Piola (2005), On the relationship between satellite retrieved surface temperature fronts and chlorophyll-a in the Western South Atlantic, *J. Geophys. Res.*, *110*, C11016, doi:10.1029/2004JC002736.

Simpson, J. H. (1981), The shelf sea fronts: Implications of their existence and behavior, *Phil. Trans. R. Soc. London, Ser. A*, *302*, 531–546.

Yoder, J. A. (2000), An overview of temporal and spatial patterns in satellite-derived chlorophyll-a imagery and their relation to ocean processes, in *Satellites, Oceanography and Society*, edited by D. Halpern, pp. 225–238, Elsevier, New York.

M. Charo, A. R. Piola, and S. I. Romero, Departamento Oceanografía, Servicio de Hidrografía Naval, Av. Montes de Oca 2124 (D1270ABV), Buenos Aires, Argentina. (apiola@hidro.gov.ar)

C. A. E. Garcia, Departamento de Física, Fundação Universidade Federal do Rio Grande, R. Eng. Alfredo Huch 475, Rio Grande (RS), 96201-900, Brazil.